Boosting visible light conversion in the confined pore space of nanoporous carbons

(Article begins on next page)

15 October 2023

iris - AperTO

Boosting visible light conversion in the confined pore space of nanoporous carbons

Alicia Gomis-Berenguer[1], Jesus Iniesta[2], Artur Moro[3], Valter Maurino[4], Joao C. Lima[3], Conchi O. Ania [1]*

[1] Instituto Nacional del carbon (INCAR,CSIC), Apdo. 73, 33080 Oviedo, Spain

[2] Institute of Electrochemistry, Faculty of Science, Univ. Alicante, 03080, Spain

[3] Dpt. Chemistry, REQUIMTE/CQFB, Faculdade de Ciências e Tecnologia, Universidade Nova de Lisboa, 2829-516 Lisboa, Portugal

[4] Department of Chimica, Università di Torino, Via P. Giuria 5-7, 10125 Torino, Italy

Abstract

We showed the outstanding effect of commensurate confinement in the pores of nanoporous carbons in the conversion of visible light into a chemical reaction. By using a series of nanoporous carbons a controlled distribution of pore sizes obtained from a gradual activation under controlled conditions we have demonstrated the superior conversion of light in the constrained pore space of the carbons compared to values in solution. Besides a more efficient conversion of light, nanopore confinement resulted in a 100-200 nm redshift in the wavelength onset of the photochemical reaction. The visible light activity was boosted in pores which sizes match the dimensions of the confined compound. We attribute this to the enhanced splitting and charge separation of the photogenerated species in the nanopores, due to the proximity of the charge carriers and the adsorbed molecules.

*Corresponding author. E-mail: conchi.ania@incar.csic.es (CO Ania)

1. Introduction

Our recent research has put forward the intrinsic photochemical activity of nanoporous carbons under adequate illumination conditions, [1,2] demonstrating their ability to photogenerate radical oxygen species (ROS) in aqueous environments [3,4]. This has opened new perspectives in the field of applied photochemistry based on carbon materials covering from photooxidation reactions for environmental remediation and photoassisted regeneration of exhausted carbon adsorbents, [5,6] to water splitting [7], enhanced adsorption/oxidation or photoluminescence [8-11]. Despite the rising interest in the field, there is still a multitude of fundamental questions that are worth investigating to exploit the potentialities of light-responsive carbons for technological applications related to the conversion of light into chemical reactions. In this regard, several authors have reported the possibility to modulate the light absorption features of nanoporous carbons upon surface functionalization, favoring the conversion of low energy photons from the visible light spectrum into chemical reactions (i.e., photoelectrochemical water splitting) by introducing N and S-containing surface groups on the carbon matrix [7, 11-14].

Aiming at throwing some light on the field, we herein show the dependence of the photochemical response of carbons with the nanopore confinement and the wavelength of the irradiation source, choosing the photooxidation of phenol as a model reaction. Conceptually, the confinement of light in constrained pore spaces has been reported to enhance light-matter interactions, allowing for instance measurements of low quantum yield photochemical reactions [15,16]. Some studies have been performed on the accommodation of photoactive guests inside the internal voids or nanocages of porous hosts (mostly for zeolites and MOFs), but yet little is known about the effects of exciton confinement in the pore structure of light-responsive carbons where the porous host exhibits strong absorption features. From a technological viewpoint, only the understanding of the fundamentals of the photochemistry of

carbons would allow a successful integration of the photo-assisted reactions based on light-responsive nanoporous carbons to a wide panel of technological processes in the near future.

2. Experimental

2.1 Materials synthesis

A series of nanoporous carbons with progressively changing pore structures were obtained from activation of coal under CO_2 atmosphere (10ºC/min up to 900ºC in 100 mL/min N_2, then switch to CO_2, 10 mL/min) for variable periods of time. The samples were labeled as F1 and F4, where the number represents the increasing burn-off degree achieved in the activation. Selected physicochemical characteristics of the samples are compiled in Table 1.

Table 1. Main physicochemical characteristics of the studied nanoporous carbons obtained from gas adsorption, chemical composition (wt.%), and surface pH.

	F	F1	F4
$S_{BET}[m^2 g^{-1}]$	799	1145	1800
$V_{PORES} [cm^3 g^{-1}]$ [A]	0.35	0.5	0.84
Porosity, $\varepsilon[\%]$ [B]	38	45	54
C (wt.%)	96.15	95.92	95.85
H (wt.%)	0.70	0.45	0.22
N (wt.%)	0.14	0.11	0.09
O (wt.%)	2.90	3.43	3.73
Surface pH	8.1	8.2	8.0

[A] Total pore volume evaluated at relative pressure of 0.99
[B] Porosity (%) evaluated from the bulk and helium densities [17]
$\varepsilon (\%) = [1- (\rho_{apparent}/\rho_{Helium})] \times 100$

2.2 Irradiation set-up and phenol photooxidation.

A Xe lamp (3000 W) coupled to a monochromator was used to irradiate the samples. The photon flux arriving at each wavelength was measured by ferrioxalate actinometry [18], and used to normalize the photochemical conversions (see Figure S1 in the Electronic Supplementary Information File, ESI). Before irradiation, suspensions of the carbons in a

phenol solution are allowed to equilibrate until all phenol is completely adsorbed; then they are irradiated for 30 min under stirring. The solution is filtered out and analyzed by reverse phase HPLC and UV-visible spectrophotometry. The carbons are further extracted with ethanol and the alcoholic solution is also analyzed to identify reaction intermediates. Extraction yields are previously determined for each pure compound and carbon. The corresponding blanks of direct degradation upon irradiation in the absence of catalyst were carried out under similar conditions. All the measurements were done at least in duplicates; average values and standard deviations are presented.

2.3 *Characterization techniques.*

The textural properties of the samples were determined by means of N_2 and CO_2 adsorption at -196 and 0ºC, in a volumetric analyzer. Before the experiments, samples were outgassed at 120 ºC overnight to constant vacuum (10^{-4} Torr). The main textural parameters such as specific surface area, S_{BET}, pore volumes and distribution of pore sizes were evaluated from the gas adsorption isotherms. The carbon materials were further characterized by elemental analysis (LECO CHNS-932 and VTF-900 automatic analyzers) and surface pH [19]. X-ray photoelectron spectra were recorded on a SPECS spectrometer with a Phoibos 100 hemispherical analyzer with a multichannel detector. The base pressure in the ultra high vacuum chamber was below 10^{-7} kPa. The X-ray radiation source was monochromatic AlKa (1486.74 eV) at 100W X-ray power and anode voltage of 14 kV. The photo-excited electrons were analyzed in constant pass energy mode, using pass energy of 50 eV for the Surrey spectra and 10 eV for the high resolution core level spectra. During data processing of the XPS spectra, binding energy values were referenced to the C 1s peak at 284.6 eV. The CasaXPS software package was used for acquisition and data analysis. A Shirley-type background was subtracted from the signals. Recorded spectra were always fitted using

Gauss–Lorentz curves, in order to determine the binding energy of the different element core levels more accurately. The error in binding energy was estimated to be ca. 0.1 eV.

2.4. Spin Trapping Electron Spin Resonance (ESR) Measurements.

The formation of paramagnetic species in solution during irradiation of the carbon suspensions was detected by a nitrone spin trapping agent (5,5-dimethylpyrroline-N-oxide, DMPO). This compound is capable of forming spin adducts with hydroxyl and superoxide radicals, creating more stable nitrone radicals that are easily detected by ESR spectroscopy in aqueous solution. About 0.5 g/L of the carbon samples were suspended in 5 ml of $HClO_4$ buffer (pH 3), and the appropriate volume of DMPO was added to the suspension to reach a final concentration of 18 mM. Samples were introduced in capillary quartz tubes and irradiated for 5, 10, 20 and 60 minutes (Philips TL K40W/05 lamp, with a broad emission peak centered at 365 nm). ESR spectra were immediately recorded from the solution (after filtering out the solids) at room temperature on a Bruker ESP 300E X band spectrometer with the following spectral parameters: receiver gain 105; modulation amplitude 0.52 G; modulation frequency 100 KHz, microwave frequency 9.69 GHz; microwave power 5.024 mW; conversion time 40.96 ms; center field 3450 G, sweep width 120 G.

3. Results and discussion

To tackle the study of the carbon/light interactions occurring inside nanoconfined pore spaces it becomes crucial to avoid other secondary reactions inherent to high energy irradiation sources and porous materials (i.e. direct photolysis and adsorption). We have developed a strategy to overcome this limitation based on evaluating the efficiency of a photochemical reaction -for instance, the photooxidation of phenol in solution- occurring in the inner void space of nanoporous materials (see scheme in ESI). The approach consists in introducing the

target compound inside the pore structure of the material (adsorbed), and illuminating the suspension in water for a predetermined time. After irradiation, both components of the suspension (solution and carbon) are analyzed to determine if there has been lixiviation to the solution (not being the case for any of the studied carbons) and the compounds still retained inside the porosity of the carbon after light exposure, using extraction in ethanol. This allows to determine the extent of the photochemical reaction that takes place inside the porosity of the material [1,2].

The starting carbon (sample F) of this study is a biomass-derived material, chosen for its photochemical activity under UV light [2] and narrow distribution of pore sizes within the micropore range. To gain additional insight on the effect of light conversion inside nanoconfined pore spaces, sample F was activated under CO_2 atmosphere for variable periods of time to obtain samples F1 and F4 with increasing burn-off degrees. It is important to highlight that during the activation reaction, the chemical composition of the carbons remained almost unaltered (Table 1), with changes exclusively seen in the pore volume, surface area and particularly the narrow microporosity. This was further confirmed by additional characterization of the samples by XPS (see discussion below) and TPD-MS (Figure S2).

Figure 1 shows the effect of the activation under strict controlled conditions on the narrow microporosity of the carbons by the analysis of the carbon dioxide adsorption isotherms [20] The isotherm of the pristine carbon F displays a concave shape characteristic of materials with a well-defined narrow microporosity; the curvature at low relative pressures becomes less pronounced with the burn-off degree, whereas at higher relative pressures the isotherms intersect each other, with the activated samples displaying larger gas uptakes. This confirms the enlargement of the micropores with the activation treatment, also evidenced by the L parameter† representing the mean pore size (inset Figure 1).

For the photochemical experiments, the carbons were loaded with a fixed amount of phenol per unit mass (ca. 0.09 mmol/g), chosen to keep the loading of phenol below the saturation limit for all three studied carbons (Figure S3). This procedure allows confining the adsorbed fraction of phenol into the narrow microporosity of the carbons [21,22]. This avoids desorption in the course of the irradiation (thus contribution of photolytic breakdown is discarded) [1,2]. It also leads to high photoconversion values, thereby minimizing any experimental error associated to the quantification of any compound in the extracts. The wavelength dependence of the photochemical activity of the carbons was determined using monochromatic light. Unlike most studies dealing with polychromatic light, this allows discriminating between the contributions of the high/low energy photons, and hence isolating any actual visible-light conversion without biased interpretations.
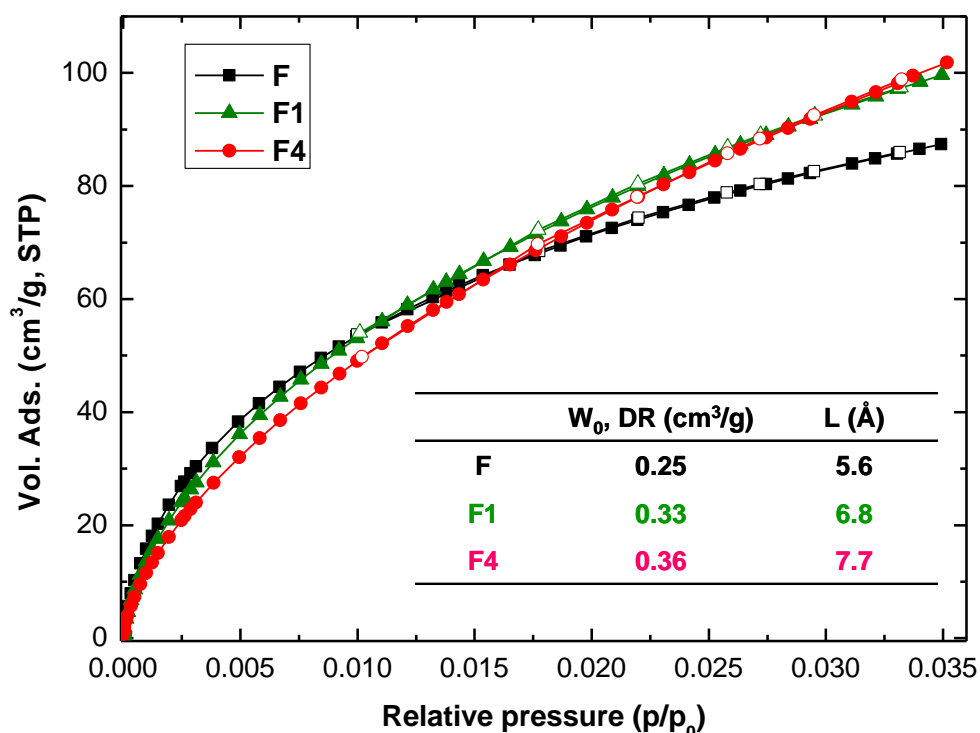
Figure 1. Carbon dioxide adsorption isotherms measured at 273 K showing the differences in the narrow microporosity of the studied carbons. Inset: micropore volume (Wo) obtained from the Dubinin Radushkevich (DR) and mean pore width (L parameter).
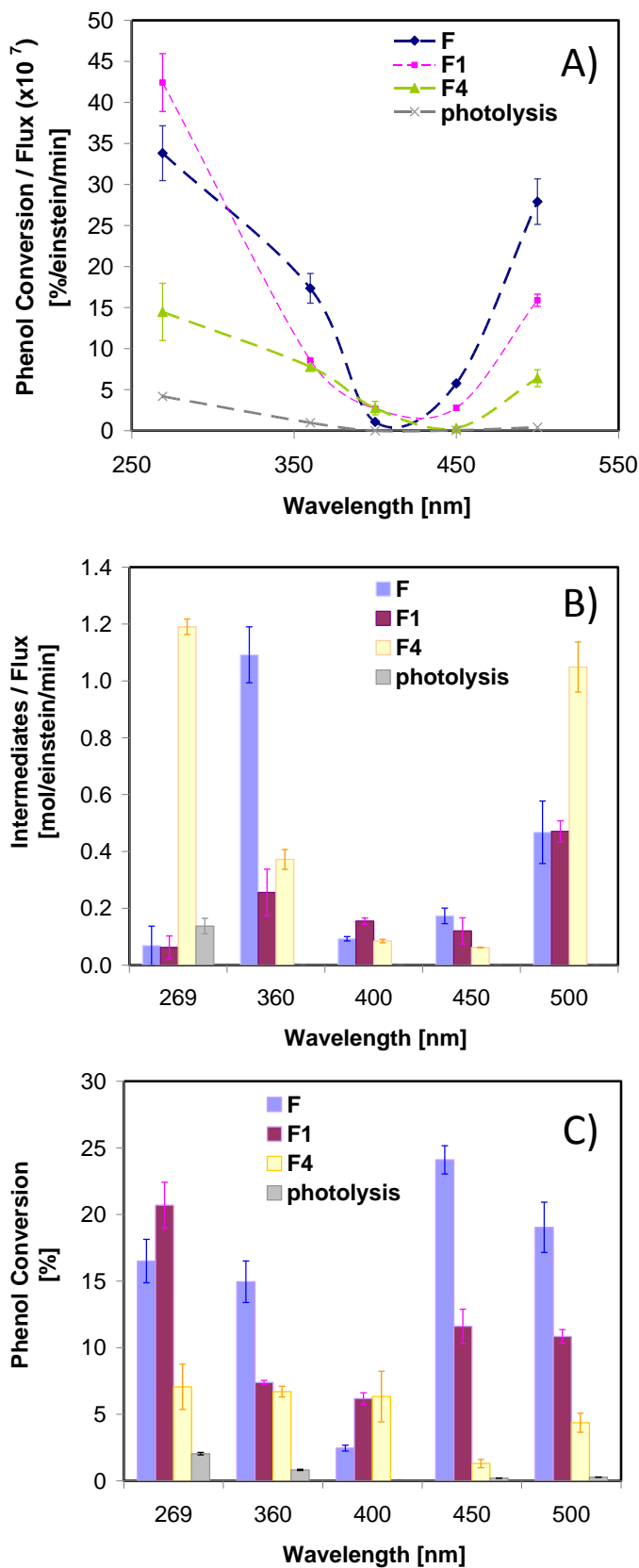
Figure 2 shows phenol conversion values (data from the extracts) upon irradiation of the pre-loaded nanoporous carbons at selected wavelengths. As the incident photon flux is different for each wavelength (Figure S1), conversion was normalized per photon flux to allow direct comparison of all data. For clarity, the actual (non-corrected) values of phenol conversion at each wavelength are also presented in Figure 2C.

The composition of the extracts after irradiation of the preloaded carbons confirmed the photoinduced degradation of phenol in the constrained pore space for all the studied samples and all selected wavelengths. This is most remarkable considering that carbons are strong light absorbers, hence a large fraction of the light is not expected to reach the molecules in the adsorbed state retained in the inner porosity. Most importantly, phenol conversion in the confined state is higher than that of direct photolysis from solution (ca. below 2%) as seen in Figure 2C, corroborating the outstanding role of nanoconfinement in enhancing the light conversion into a chemical reaction. Also, whereas direct photochemical breakdown of phenol from solution is negligible at wavelengths above 300 nm, outstanding conversion values are obtained at 450 and 500 nm when the photochemical reaction was carried out inside the confined pore space. This corresponds to over 100-200 nm redshift in the wavelength onset for the photochemical reaction compared to photolysis in solution, and clearly demonstrates the ability of nanoporous carbons to convert sunlight into a chemical reaction.

Interestingly, the photochemical performance followed a U-shaped pattern rather than a decreasing trend with the wavelength (Figure 2A). All three carbons showed a minimum at 400 nm, derived from very low conversion values (Figure 2C), whereas at wavelengths corresponding to visible light (i.e., 450 and 500 nm), the conversion rose again with values very close to those obtained at 269 nm. In our previous studies we also observed low conversion values at 400 nm using a different lamp set-up, and tentatively attributed this to the low photon flux provided by the source, rather than to the inactivity of the carbon

materials [1]. This hypothesis however would not apply to these systems since the incident photon flux at 400 nm is several times higher than those measured for the rest of the wavelengths (Figure S1). Yet the conversion values at 400 nm are much lower than those of the other wavelengths in the series.

Interesting features are revealed for the wavelength dependence of the photooxidation yields with the activation treatment. Despite all three carbons showed a similar wavelength onset of the photochemical activity -in agreement with the performance described for other nanoporous carbons in our earlier works- [1], we herein report the correlation of these differences in conversion with the confinement state of the adsorbed molecules. Phenol conversions (Figure 2) followed the general trend: F >F1>F4, with larger differences at higher energy photons (lower wavelengths), demonstrating a more successful exploitation of light in tight confinements. Only the performance at 269 nm slightly escapes from this trend, as the photochemical conversion of F and F1 is rather alike. The amount of degradation intermediates (dihydroxylated benzenes) also depends on the confinement and the illumination conditions (Figure 2B). At 269 nm both phenol and its aromatic intermediates are efficiently decomposed, whereas as the irradiation becomes less energetic the amount of intermediates gradually increases -conversion of phenol does not follow the same trend-; this points out that the photooxidation reaction is hindered or delayed to some extent, likely due to the difficulty in pursuing the oxidation of dihydroxylated compounds under visible light.

Figure 2. A) Phenol conversion and B) amount of degradation intermediates (dihydroxylated

benzenes) per incident flux at different wavelengths on all three studied carbons; C)

actual (non-corrected) phenol conversion values at each wavelength.

The dependence of the yield of the photochemical reaction with the average pore size at different wavelengths is more clearly seen in Figure 3. As a general trend, the photochemical conversion of phenol gradually decreased with the enlargement of the average pore size, being the effect less remarkable at large wavelengths. Data also showed a wavelength dependent threshold pore size for an optimum exploitation of the light. At 269 nm the conversion of light was enhanced for pores below 7 Å (with small differences between them) whereas the photochemical response was drastically reduced when the pores is widened by 1Å. For higher wavelengths, the drop in the photochemical conversion is very pronounced, particularly at 500 nm where the performance is quite close to that of 269 nm for pore apertures of 5.6 Å.

To understand this behaviour we must consider the confinement state of the adsorbed molecules in the constrained pore space. As mentioned above, the amount of phenol incorporated in the pores was below the saturation limit of the carbons to restrict the confinement of the adsorbed molecules to the narrow microporosity (molecular dimensions of phenol are ca. 0.80 x 0.67 x 0.15 nm) in single adsorption layers (maximizing host-guest interactions). According to literature [21,22], adsorption of phenolic derivatives on hydrophobic carbons is governed by dispersive interactions with phenol molecules predominantly adsorbed in an edge-wide orientation, with the aromatic ring parallel to the pore walls (plane-on) and the hydroxyl moiety projecting away from pore walls towards the aqueous phase [23].

On the other hand, the light absorption features of amorphous carbons depend on the density of electronic states, DOS, (mainly sp^2/sp^3 hybridization of the carbon atoms), and in the UV range are dominated by $\pi-\pi*$ and $\sigma-\pi*$ transitions involving free zig-zag sites and carbine-like sites [24-26]. Under sunlight irradiation, some other transitions involving the activation of chromophoric groups on the carbon surface have been proposed [7-9, 27]. Considering the

low and quite similar functionalization of these carbons (Table 1), we expect the latter contribution to be small.
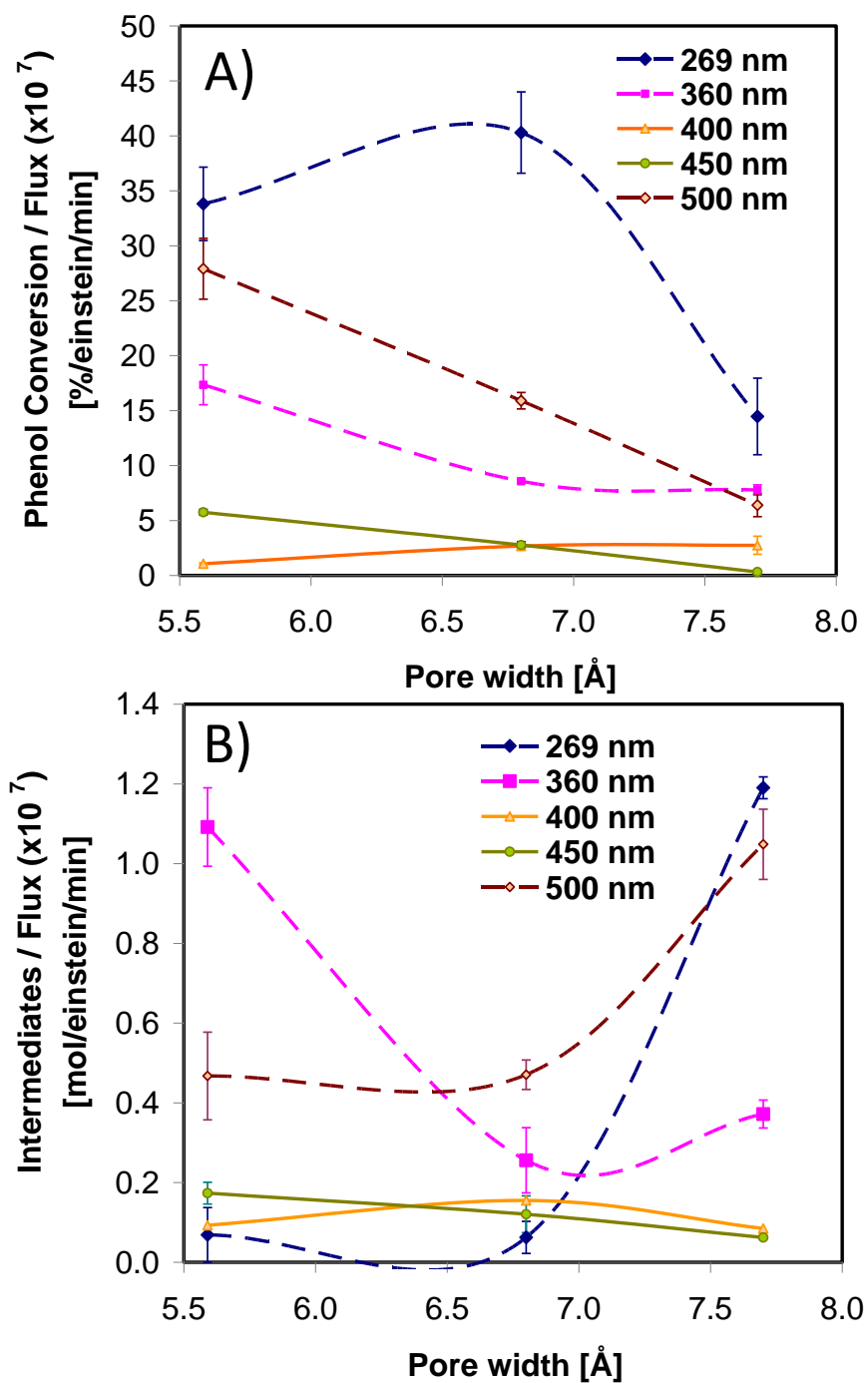
Figure 3. Correlation of normalized phenol photoxidation conversion (A) and intermediates detected (B) with the pore size at different wavelengths.

Hence, irradiation of the carbons gives rise to the formation of excitons (holes or electrons), which when splitting is favoured can participate in charge transfer reactions with electron donors present in the reaction medium [28,29]. The superior conversion of the carbons compared to the photolytic reaction confirms that the light conversion is boosted in the constrained pore space, and the differences for the three materials point out the role of confinement.
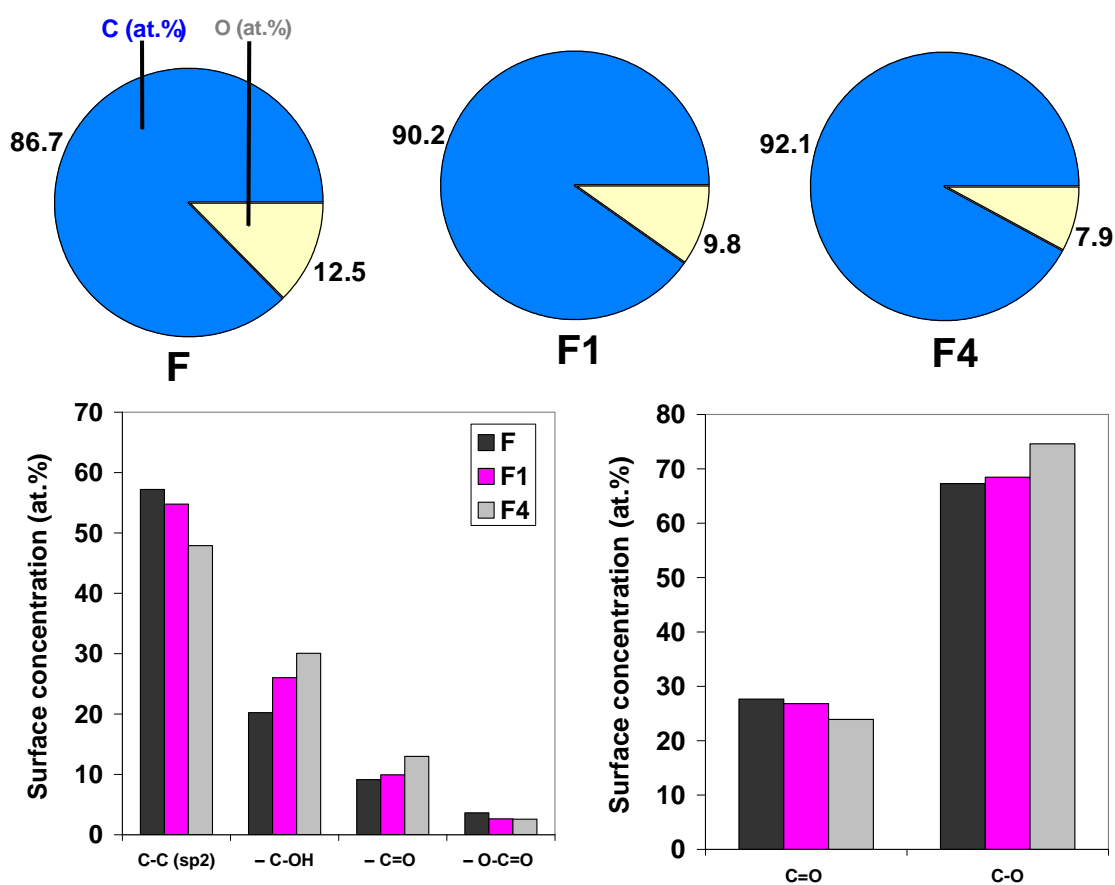

Figure 4. Surface concentration (atomic %) of heteroatoms (top) and distribution of carbon and oxygen species (down) obtained by fitting the C 1s and O 1s core level peaks of XPS spectra.

In this regard, the characterization of the carbons confirmed the smooth CO_2 activation treatment affecting mostly the enlargement of the micropores (Figure 1). Indeed, no significant changes were detected either on the surface functionalization of the activated samples, the disorder degree derived from the removal of carbon atoms at the edges-, or inducing structural defects due to modifications in the sp^2/sp^3 hybridization of carbon atoms (Figure 4). All of these would eventually have a strong effect in the optical characteristics (ca. creation of distorted sites in the DOS) of the carbons, and the stabilization of the photogenerated carriers through the delocalization within the conjugated sp^2 network of the basal planes.

On the contrary, differences must be attributed to the fate of the charge carriers in the constrained pore space. The tight confinement of phenol molecules in pores that commensurate the molecular size facilitates the exciton splitting through the reaction with electron donors, boosting the conversion of light. Several scenarios might be plausible; the first one is that the holes might directly react with the adsorbed phenol molecules, as the on-plane orientation favours the proximity of the π electrons of the aromatic ring towards the pore walls where the exciton is generated (however we do not have direct evidence for this).

Another possibility is the stabilization of the holes through the oxidation of water molecules co-confined in the pores along with phenol to form hydroxyl radicals. This is supported by the detection of ROS after irradiation of aqueous suspensions of the carbons using spin resonance spectroscopy and nitrones as spin trapping chemicals (Figure 5). The photogeneration of hydroxyl radicals for all the carbons corroborates the separation of the exciton and migration to the aqueous solution. When phenol is introduced inside the nanopores, the radicals are more efficiently used for the photooxidation of the adsorbed molecules, as corroborated by the nature of the intermediates detected (namely dihydroxylated benzenes).
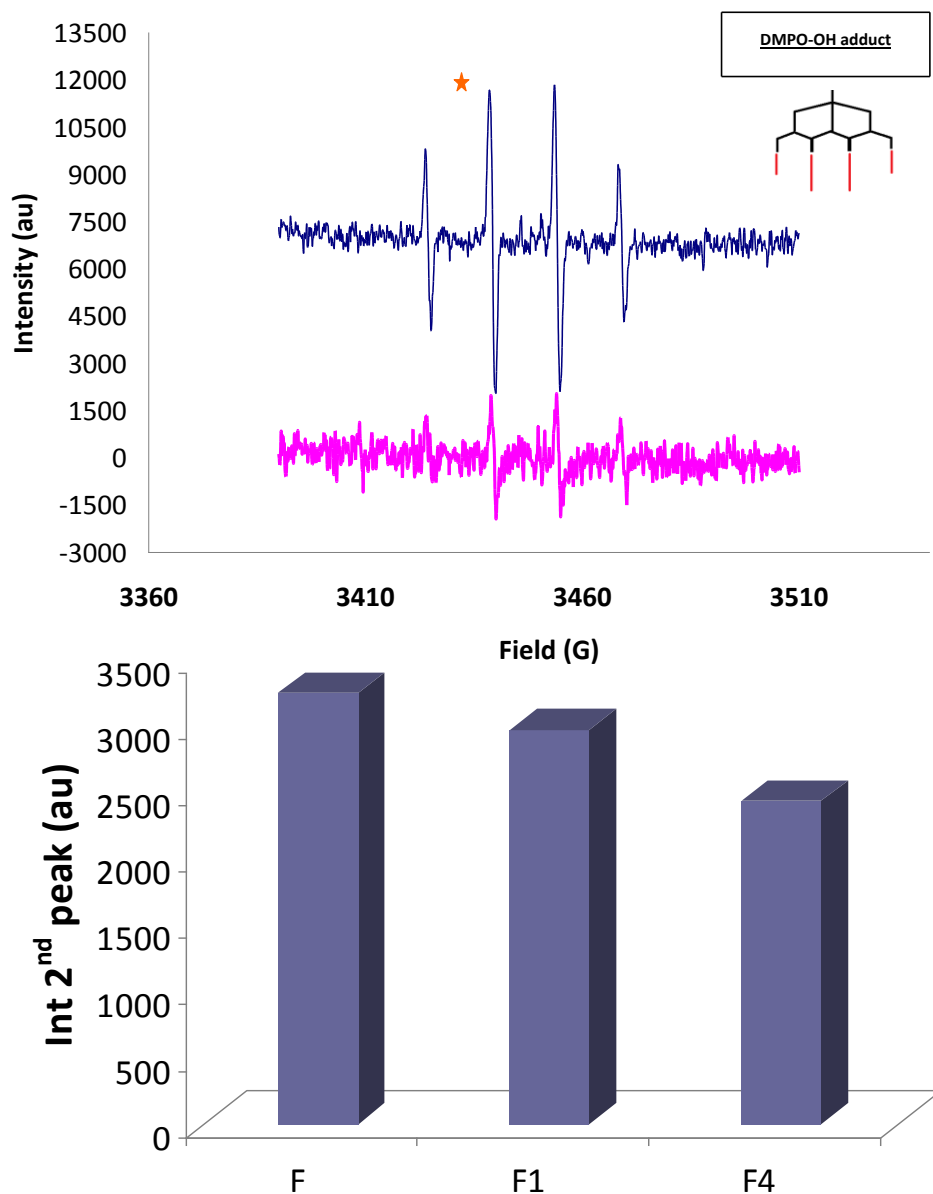
Figure 5. (top) Characteristic ESR signal of DMPO-OH adduct obtained upon 20 minutes of irradiation of aqueous suspensions of a nanoporous carbon and titania powders for comparison. (down) Quantification of the radical species detected from the ESR signals corresponding to DMPO-OH adducts by integration of the second peak in the 1:2:2:1 quartet profile (marked as *).

CONCLUSIONS

We report the superior conversion of light into a chemical reaction boosted in the constrained pore space of nanoporous carbons. Matching of the molecular dimensions of the target compound confined in the carbon pore network results in a 100 nm red-shift of light conversion. As a result, the proximity between the photogenerated charge carriers and the adsorbed molecule in the constrained pore space facilitates the exciton splitting and the charge separation, enhancing the conversion of the photooxidation reaction under both UV and sunlight.

We anticipate that tuning the porous network of nanoporous carbons with photochemical activity opens up an interesting strategy to master the conversion of light in chemical reactions, especially favoring the utilization of sunlight. The control of the pore structure of nanoporous carbons is no longer a challenge, which offers an interesting opportunity to improve light harvesting through the control of the physicochemical features of low cost porous carbons to facilitate exciton splitting.

Owing to the recently gained interest on the use of carbon materials in photochemical applications and their versatility of forms, structures and precursors, our findings demonstrate that it is highly feasible to push the use of nanoporous carbons as sustainable metal-free and low cost photoactive materials, particularly when much attention is lately being paid to the investigation of more sophisticated forms of carbons (graphene, nanotubes, graphite oxide), so far considered non photoactive under visible light.

The challenge still remains in the further enhancement of the photochemical activity by balancing the surface composition, porosity, and change-carrier mobility. The dependence of the photochemical activity of the studied carbons with the nanopore confinement described here is expected to be valuable in general for targeting other applications in the fields of solar

energy conversion (e.g. water splitting, carbon photofixation reactions, photovoltaic devices) on light responsive carbons.

REFERENCES

[1]   Velasco LF, Lima JC, Ania CO. Visible-light photochemical activity of nanoporous carbons under monochromatic light. Angew. Chem. Int. Ed. 2014; 53:4146-4148.

[2]   Velasco LF, Parra JB, Fonseca IM, Lima JC, Ania CO. Photochemical behaviour of activated carbons under UV irradiation. Carbon 2012; 50:249-258.

[3]   Velasco LF, Maurino V, Laurenti E, Fonseca IM, Lima JC, Ania CO. Photoinduced reactions occurring on activated carbons. A combined photooxidation and ESR study. Appl. Catal. A General 2013; 452:1-8.

[4]   Velasco LF, Maurino V, Laurenti E, Ania CO. Light-induced generation of radicals on semiconductor-free carbon photocatalysts. Appl. Catal. A General 2013; 453:310-315.

[5]   Velasco LF, Carmona RJ, Matos J, Ania CO. Performance of activated carbons in consecutive phenol photooxidation cycles. Carbon 2014; 73:206-215.

[6]   Velo-Gala I, Lopez-Peñalver JJ, Sanchez-Polo M, Ribera-Utrilla J. Activated carbon as photocatalyst of reactions in aqueous phase. Appl. Catal. B 2013; 142: 694-704.

[7]   Ania CO, Seredych M, Rodriguez-Castellon E, Bandosz TJ. Visible light drieven photoelectrochemical wáter splitting on metal free nanoporous carbon promoted by chromophoric functional groups. Carbon 2014; 79:432-441.

[8]   Bao L, Zhang ZL, Tian ZQ, Zhang L, Liu C, Lin Y, Qi B, Pang DW. Electrochemical tuning of luminescent carbon nanodots: From preparation to luminescence mechanism. Adv. Mater. 2011; 23:5801-5806.

[9]   Bao Q, Zhang J, Pan C, Li J, Li CM, Zang J, Tang DY. Recoverable photoluminescence of flame-synthesized multiwalled carbon nanotubes and its intensity enhancement at 240K. J. Phys. Chem. C 2007; 111:10347-10352.

[10] Bandosz TJ, Rodriguez-Castellon E, Montenegro JM, Seredych M. Photoluminescence of nanoporous carbons: Opening a new application route for old materials. Carbon 2014; 77:651-659.

[11] Seredych M, Messali L, Bandosz TJ. Analysis of factors affecting visible and UV enhanced oxidation of dibenzothiophenes on sulphur-doped activated carbons. Carbon 2013; 62:356-364.

[12] Pan D, Zhang J, Li Z, Wu M. Hydrothermal route for cutting graphene sheets into blue-luminescent graphene quantum dots. Adv. Mater. 2010; 22:734-738.

[13] Bandosz TJ, Matos J, Seredych M, Islam MSZ, Alfano R. Photoactivity of S-doped nanoporous activated carbons: A new perspective for harvesting solar energy on carbon-based semiconductors. Appl. Catal. A 2012; 445:159-165.

[14] Seredych M, Bandosz TJ. Effect of the graphene phase presence in nanoporous S-doped carbon on photoactivity in UV and visible light. AppL. Catal. B 2014; 147:842-850.

[15] Li B, Li F, Bai S, Wang Z, Sun L, Yang Q, Li C. Oxygen evolution from water oxidation on molecular catalysts confined in the nanocages of mesoporous silicas. Energy Environ. Sci. 2012; 5:8229-8233.

[16] Corma A, Garcia H. Zeolite-based photocatalysts. Chem Comm. 2004:1443-1459.

[17] Rouquerol F, Rouquerol J, Sing KSW, Llewellyn P, Maurin G. Adsorption by Powders, Porous Solids Principles, Methodology, Applications. 2nd ed. Elsevier; 2014.

[18] Kuhn HJ, Braslavsky SE, Schmidt R. Chemical actinometry. Pure Appl. Chem. 2004; 76:2105-2146.

[19] Noh JS, Schwarz JA, Estimation of the point of zero charge of simple oxides by mass titration, J. Colloid Interface Sci. 1989; 130: 157-164

[20] Lozano-Castelló D, Cazorla-Amorós D, Linares-Solano A. Usefulness of CO_2 adsorption at 273K for the characterization of porous carbons. Carbon 2004; 42: 1233-1442.

[21] Velasco LF, Ania CO. Understanding phenol adsorption mechanisms on activated carbons. Adsorption 2011; 17:247-254.

[22] Radovic LR, Moreno-Castilla C, Rivera-Utrilla J. Chemistry, Physics of Carbon. Radovic LR, New York: Marcel Dekker; 2000:227-405.

[23] Singh DD. Surface orientation of phenol molecules adsorbed from aqueous-solution by carbon-blacks, Ind. J. Chem. 1971; 9:1369.

[24] Modestov AD, Gun J, Lev O. Graphite photelectrochemistry study of glassy carbon, carbon-fiber and carbon-black electrodes in aqueous electrolytes by photocurrent response. Surf. Sci. 1998; 417:311-322.

[25] Robertson J. Mechanical properties and coordinations of amorphous carbons. J. Phys. Rev. Lett. 1992; 68:220-223.

[26] Radovic LR, Bockrath B. On the chemical nature of graphene edges: Origin of stability and potential for magnetism in carbon materials. J. Am. Chem. Soc. 2005; 127:5917-5927.

[27] Ocampo-Pérez R, Sánchez-Polo M, Rivera-Utrilla J, Leyva-Ramos R. Enhancement of the catalytic activity of TiO_2 by using activated carbon in the photocatalytic degradation of cytarabine. Appl. Catal. B Envir. 2011; 104:177-184.

[28] Zhao Y, Nakamura R, Kamiya K, Nakanishi S, Hashimoto K. Nitrogen-doped carbon nanomaterials as non-metal electrocatalysts for water oxidation. Nature Comm. 2013; 4:2390.

[29] Jana D, Sun CL, Chen LC, Chen KH. Effect of chemical doping of boron and nitrogen on the electronic, optical, and electrochemical properties of carbon nanotubes. Prog. Mater. Sci. 2013; 58:565-635.